Thesis Title

A DISSERTATION
SUBMITTED TO THE FACULTY OF THE GRADUATE SCHOOL
OF THE UNIVERSITY OF MINNESOTA
BY

Vladimir Bychkov

IN PARTIAL FULFILLMENT OF THE REQUIREMENTS
FOR THE DEGREE OF
DOCTOR OF PHILOSOPHY

Gregory Pawloski

..., 2018

Acknowledgements

There are many people that have earned my gratitude for their contribution to my time in graduate school.

Dedication

To those who held me up over the years

Abstract

Contents

List of Tables

List of Figures

Chapter 1

Introduction

The goal of this work is to study and understand properties of one of the most mysterious elementry particles in the universe - neutrinos. Neutrino is chargeless and has mass which is less by many orders of magnitude than masses of others fundamental particles. It is known that neutrinos could interact only through weak and gravitational forces which leads to a several light years of mean free path in the matter. Despite their tiny mass and weak interaction with the matter, they are very interesting not only to elementary particle physics community but also to cosmologists and astrophysicists. Neutrinos carry away almost all energy of supernova explosion and can tell a lot about a dying star's internal structure and the last seconds of its life. Neutrino telescopes may open a new window for Universe observation and give a unique look into phenomena which could not be seen by conventional telescopes. These light, electrically neutral particles also can show physicists a possible direction towards new physics. The list of examples why neutrinos are important continues to grow, and it gives a sense that neutrino physics is a very rich and interesting subject to study.

In addition, neutrinos take part in one more fascinating phenomenon called neutrino oscillations. While produced in one flavour after travel some distance neutrino is changing its flavour to another one in an oscillatory way. The NOvA - NuMI[1] Off-axis Neutrino Appearnace - experiment was designed to study properties of these oscillations.

[1] Neutrino at the Main Injector

There are several parameters which fully describe neutrino oscillations and analysis presented in this work is focused on measuring $\sin^2\theta_{23}$ and $|\Delta m^2_{32}|$. The measurements come from studying a specific mode of the oscillations: $\nu_\mu \to \nu_\mu$.

Here is a brief outline of the work

- Chapter 2 briefly presents the history of neutrino discovery and observation of neutrino oscillations.
- Chapter 3 discusses corresponding theory behind the neutrino oscillation physics together with the current measurements of the parameters describing these oscillations.
- Chapter 4 describes the NOvA experiment design and its two most significant parts - Far and Near Detectors.
- Chapter 5 provides details on Monte Carlo simulations used in the analysis.
- Chapter 6 follows the reconstruction chain from raw data to high level objects such as slices, tracks etc. Energy estimation algorithm is considered.
- Chapter 7 .... hashes out the strategy for analysis and presents the data and simulated sets that will be used in the analysis.
- Chapter 8 discusses event selection and background reduction processes for the contained and uncontained samples.
- Chapter 9 gives predictions for selected events in Far Detector
- In Chapter 10 all the systematics are discussed.
- Chapter 11 presents a final discussion of the analyses presented in the thesis.

Chapter 2

Neutrino and its oscillation

2.1 History of neutrino discoveries

The energy spectrum of beta decay electrons was accurately measured by James Chadwick in 1914 [2]. Previous attempts by Lise Meitner and Otto Hahn in 1911 and Jean Danysz in 1913 showed hints that the electron energy spectrum was continuous. At the time this was an obvious contradiction with laws of energy and angular momentum conservation. A nucleus emitting an electron changes its state and energy of the electron should be equal to the energy difference of two nucleus' states. After several attempts to explain the mystery of beta decay Wolfgang Pauli postulated [3] that beta decay is actually a three particle decay. He called the third particle "neutron" - an electrically neutral and very light particle - and it was responsible for carrying away some portion of the energy which leads to continuous electron energy spectrum. Two years later in 1932 an actual neutron - the proton's partner inside a nucleus - was discovered by Chadwick [4]. To avoid confusion Enrico Fermi proposed a new name for Pauli's particle [5] - neutrino, which means "little neutral one".

It took more than 20 years for the first neutrino to be observed. In 1956 Reines and Cowan made a direct observation of a neutrino [6], whose flavor was later recognized as an electron anti-neutrino $\bar{\nu}_e$. An anti-neutrino was produced in a nuclear fission reactor via neutron decay

$$n \rightarrow p + e^- + \bar{\nu}_e. \tag{2.1}$$

An anti-neutrino interacted with a proton in a detector and produced positron and neutron

$$\bar{\nu}_e + p \rightarrow e^+ + n. \tag{2.2}$$

A signature of both processes, and thus evidence of the neutrino, was observed by a detector in the following way. An anti-neutrino interacted with a proton to produce a positron and neutron. The positron annihilated with an electron and produced two photons. Shortly after the neutron was captured by a nucleus and emitted another photon. Two photons followed by a third one gave an indication of a neutrino interaction inside the detector. For the detection of the neutrino the Nobel Prize was awarded to Reines in 1995.

In 1962 the neutrino family was expanded by observation of the second type of neutrino - a muon neutrino ν_μ. Leon Lederman, Melvin Schwartz, and Jack Steinberger used the world's largest accelerator at Brookhaven National Laboratory to direct protons into fixed target in order to produce charged pions. Those pions subsequently decayed to (anti)muons and muon (anti)neutrinos. At the end of pion decay pipe plates made of steel and lead were installed to absorb muons. Beyond the metal absorbers a spark chamber was placed where neutrino interactions similar to (2.2) occurred,

$$\nu_\mu + n \rightarrow \mu^- + p, \qquad \bar{\nu}_\mu + p \rightarrow \mu^+ + n. \tag{2.3}$$

After processing all experimental data 34 muon neutrino interactions were found with a single muon track in the spark chamber [7]. In 1988 the group was awarded the Nobel Prize for their discovery of the muon neutrino.

The discovery of weak gauge bosons at CERN by UA1 and UA2 collaborations [8], [9] in 1983 provided new ways to study particles interacting via weak bosons. Careful measurements of the Z boson decay rates helped to establish the total number of neutrinos which interact through $W^\pm$ and Z bosons. ALEPH detector on the Large Electron Positron collider at CERN determined [10] in 1989 that only three different neutrinos participate in weak interactions. Sterile neutrinos, which do not interact weakly, are still not ruled out and searches are on going.

ALEPH experiment had suggested that a third neutrino should be associated with the tau lepton which was discovered in 1975 [11]. The Direct Observation of Nu Tau

(DONUT) experiment was setup at Fermilab in 2000 and looked for reactions

$$\nu_\tau + n \to \tau^- + p, \qquad \bar{\nu}_\tau + p \to \tau^+ + n. \tag{2.4}$$

The general idea of the DONUT experiment was similar to the experiment conducted at Brookhaven National Lab in the early 1960s. A proton beam was directed into a fixed target resulting in a shower of meson and baryons. In order to decrease the background of ν_μ neutrinos deflecting magnets were installed along the decay pipe to remove muons which produce ν_μ neutrinos upon decaying. Tau neutrinos were produced by the $D_S \to \tau + \nu_\tau$ process, and as many as 4 tau neutrino interactions were observed [12]. This number of interactions was sufficient to confirm the existence of the tau neutrino.

2.2 Neutrino oscillations

The first idea of neutrino oscillations appeared in the work of Bruno Pontecorvo in 1957 [13]. Even though at the time only one neutrino flavor was known, Bruno described the mixing of electron neutrinos and antineutrinos. Later when the muon neutrino was discovered the physicists Maki, Nakagawa, and Sakata used Pontecorvo's framework [14] to describe oscillations of neutrino flavor. After the discovery of the tau neutrino, a third neutrino was added to the oscillation picture.

Before Ray Davis and collaborators' observation of solar neutrino deficit in the 1960's [15], neutrino oscillations were considered possible but hardly realistic. Using the standard solar model the total number of electron neutrino coming from the sun was predicted by John Bahcall [16]. However, an obvious deficit of solar neutrinos was observed. Later, more advanced observations of solar neutrino flux were conducted in Japan - Super-Kamiokande [17], and in Sudbury Neutrino Observatory [18]. Both observations matched prior measurements, but contradicted predictions. This solar neutrino problem is eloquently explained in the framework of neutrino oscillations. In the following section a theoretical description of neutrino oscillations will be given.

Chapter 3

Physics of Neutrinos

3.1 Standard Model in a nutshell

Since ancient times people were trying to understand the world around them. From first world models of ancient Greeks to modern theories scientists tried to use limited number of entities to decribe phenomena happened in nature - Democritus's indivisible atoms, Plato's elements (air, fire, water, earth) or elementary particles of the Standard Model. We do not have enough time to go over all theories but rather we concentrate on the latest and the most accurate one called Standard Model.

Elementary particles of the Standrar Model are building blocks and glue of everything we can see around us[1]. However, the most fascinating thing about the Model is that underlying principles which governs it are principles of symmetry, namely, gauge symmetry and Lorentz symmetry. The Standard Model's group is

$$SU(3) \times SU(2) \times U(1), \tag{3.1}$$

where group $SU(3)$ describes strong interactions and $SU(2) \times U(1)$ describes electroweak interactions[2]. The different mathematical properties of the groups naturally split

[1] As of today, Standard Model and Einstein's General Theory of Relativity could not fully explain motion of galaxies and exponential expansion of the Universe. Two more entities were introduced - dark matter for former phenomenon and dark energy for latter one.

[2] Gravitational interaction falls out of the picture since for the last one hundred years gravity is described by deformation of space-time continium. Nevertheless, the attempts to rewrite gravity using the same language of groups and unified it with Standard Model never were given up. In fact, all latest

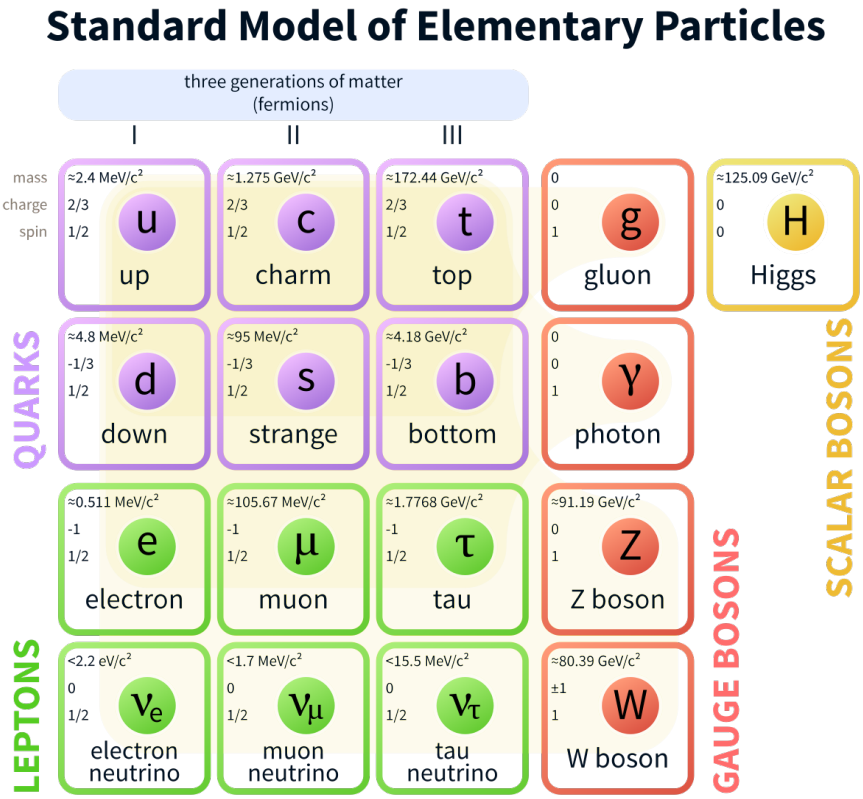

Figure 3.1: Elementary Particles in the Standard Model.
All particles could be divided into 2 groups: fermions and bosons. Fermions are further divided into quarks with fractional charges and leptons - charged ones (e, μ, τ) and neutral $(\nu_e, \nu_\mu, \nu_\tau)$. All the fermions participate in strong, weak and (only charged ones) electromagnetic interactions. These interactions are mediated by massless gluons (g), massive weak bosons $W^{\pm}$ and Z^0 and massless photon (γ). The Higgs boson is last discovered particle and is reponsible all others particles' masses.

the particles into two categories based on their spins: bosons and fermions. Fermions are particles with half-integer spin and bosons are particles with integer spin (in units of $\hbar$). The matter consists of fermions while bosons serve for carrying interactions between matter particles.

Fermions in the Standard Model are represented by quarks and leptons. Quarks make up protons and neutrons and have fractional charge - up, charm and top quarks have charge $+\frac{2}{3}e$, while down, strange and bottom have $-\frac{1}{3}e$. Quarks also have strong charge - color - which could be one of three optins: green, red or blue. The interesting fact is that the quarks are not observable in the same sense as electrons could be observable and only three (baryon) or two-quark (meson) combinations exist[3]. This phenomenon is called quark confinement with no complete explanation as of today.

The other sector of the Standard Model - lepton sector - cosnists of negatively charged electron, muon and tau particles as well as neutral neutrinos. These particles participate only in weak and electromagnetic interactions. Moreover, electron and electron neutrino posses an electron lepton number, similar for muon and tau. Lepton numbers are known to be conserved in every process, for example, muon decay produces not only electron but corresponding muon neutrino and electron antineutrino. Although attempts to observe lepton number violation are being made.

As can be seen from the figure (3.1) fermions are splitted into three generations. The mass of each subsequent generation is bigger by at least two orders of magnitude. The matter we observe around us is made of particles from first generation. Why do other generations exist? Why are there only three generations at all? Physicists do not know the answer to this questions yet as well as to the question of gigantic (10^{11}) mass difference between the lightest and the heaviest particles.

The last but not the least sector of the Standard Model is boson sector. This sector is represented by particles which mediate electromagnetic, weak and strong interactions. The photon (γ) is spin-1 massless electromagnetic force carrier and is reponsible for almost all phenomena a person experiences in his/her life - from the Sun's light to the frictions and atoms bounds in chemical elements. Only charged particles interact through photon exchange.

---

unified theories were based on groups of high demenstions where one of the most promising theories is String Theory.

[3]Recently, five quark combinations have been discover

The strong force carrier is spin-1 massless gluon (g). Gluon exchange makes quarks to be tightly bound inside baryons - protons, neutron etc - or mesons - π, ρ etc. While photon is electrically neutral and can not interact directly with other photons gluon is carrying color or rather color-anticolor and can interact with other gluons. As mentioned above only specific combinations of quarks are observable - colorless combinations - three quarks of different colors or quark-antiquark pair with color-anticolor charge. In strong interaction quark changes its color by emitting gluon, for example, a blue quark emits blue-antired gluon and becomes a red quark.

The weak force carriers are spin-1 massive $W^{\pm}$ and Z^0 bosons. All the Standard Model fermions could interact via weak bosons exchange. The weak interaction plays a major role in radiodecays and is the only way to study neutrinos since these particles do not participate in strong or electromagnetic interactions.

Among Standard Model interactions only electromagnetic one has an infinite range while others are short range interactions due to massive (weak) and color charged (strong) force carriers. The relative strength of interactions are not very meaningful as it depends on energies one uses for measurements but still can provide useful information. Strong, electromagnetic and weak interactions relate to each other as $1 : 10^{-3} : 10^{-16}$.

The masses and couplings are free parameters of the Standard Model and could be choosen in a such way that theory's predictions match observations. The fact that weak bosons have masses makes it hard to incorporate them into the theory based on gauge symmetry. However, Higgs mechanism does it in an elegant way by introducing one more entity - Higgs field - and a corresponding carrier - Higgs boson. Higgs boson is the last particle of the Standard Model and the only one with spin-0.

In addition, each particle has an antiparticle with the same mass and spin but opposite charge. Interaction of the particle and its antiparticle leads to annihilation with two photons being emmitted. It is known that our Universe consists primarily of matter and not antimatter[4]. Why did that happen during the early uuniverse is a mystery for now, however, CP-symmetry[5] violation is partially responsibble for this and NOvA experiment can shed some light on the problem.

[4]What to call matter and what antimatter is an arbitrary choice.

[5]Charge-Parity symmetry - $q \to -q, \quad \vec{r} \to -\vec{r}$.

3.2 Oscillations in Vacuum

Neutrinos are massive elementary particles which participate in weak interactions and are immune to electromagnetic and strong interactions. They also participate in gravitational interactions, but since gravity is many orders of magnitude smaller in comparison to other forces one can neglect gravity effects completely, at least on energy scale of modern experiments. There are three types of neutrinos - with definite flavor - electron (ν_e), muon (ν_μ) and tau (ν_τ) neutrinos. These flavor neutrinos are eigenstates of the weak Hamiltonian and they can be produced or destroyed only in weak interactions via exchange of the weak gauge bosons $W^\pm$ and Z. The neutrino mass eigenstates do not coincide with flavor eigenstates, and this leads to neutrino oscillations.

As was mentioned before flavor neutrinos are produced in weak interactions, but mass eigenstates are responsible for neutrino propagation through space. One can decompose the flavor eigenstates ($|\nu_e\rangle$, $|\nu_\mu\rangle$, $|\nu_\tau\rangle$) into linear combinations of mass eigenstates ($|\nu_1\rangle$, $|\nu_2\rangle$, $|\nu_3\rangle$).

$$|\nu_f\rangle = \sum_{f=e,\mu,\tau} U_{fi}|\nu_i\rangle. \tag{3.2}$$

The matrix U_{fi} is a 3×3 unitary matrix and is called the lepton mixing matrix or PMNS (Pontecorvo, Maki, Nakagawa, Sakata) matrix. U_{fi} encodes the neutrino mixing parameters such as θ_{12}, θ_{13}, θ_{23} and phase δ which is responsible for CP violation in weak interactions. The convenient parametrization is as follows:

$$U_{fi} = \begin{pmatrix} c_{12}c_{13} & s_{12}c_{13} & s_{13}e^{-i\delta} \\ -s_{12}c_{23} - c_{12}s_{23}s_{13}e^{i\delta} & c_{12}c_{23} - s_{12}s_{23}s_{13}e^{i\delta} & s_{23}c_{13} \\ s_{12}s_{23} - c_{12}c_{23}s_{13}e^{i\delta} & -c_{12}s_{23} - s_{12}c_{23}s_{13}e^{i\delta} & c_{23}c_{13} \end{pmatrix}, \tag{3.3}$$

where $c_{ij} = \cos(\theta_{ij})$ and $s_{ij} = \sin(\theta_{ij})$.

Quantum mechanics governs how mass eigenstates propagate through space. Using the Schrodinger equation $-i\hbar\frac{\partial}{\partial t}|\psi\rangle = H|\psi\rangle$ one can derive a solution for neutrino wave function at the point (x,t) of space-time starting with the wave function at the point

$(0,0)$. Using the free Hamiltonian for neutrino mass eigenstates one derives [6]

$$|\nu_i(x,t)\rangle = e^{-i(E_i t - p_i x)}|\nu_i(0,0)\rangle. \tag{3.4}$$

Neutrino masses m_i are much less in comparison neutrino energy in all experiments and the next ultra-relativistic approximation could be used

$$p_i = \sqrt{E_i^2 - m_i^2} \approx E_i - \frac{m_i^2}{2E_i}, \tag{3.5}$$

moreover, in this limit neutrino travels almost at the speed of light, so final solution for neutrino wave function with the mass m_i is

$$|\nu_i(L)\rangle = e^{-i\frac{m_i^2}{2E}L}|\nu_i(0)\rangle, \tag{3.6}$$

where L is distance which the neutrino traveled.

If one creates a neutrino of flavor f at $t = 0$ and energy E then the probability that at the distance L from the neutrino source one observes a neutrino with flavor f' is

$$\begin{aligned} P_{\nu_f \to \nu_{f'}}(L,E) &= |\langle \nu_f(0)|\nu_{f'}(L)\rangle|^2 \\ &= \Big|\Big(\sum_i \langle \nu_i(0)|U_{fi}^*\Big)\Big(\sum_{i'} e^{-i\frac{m_{i'}^2}{2E}L} U_{f'i'}|\nu_{i'}(0)\rangle\Big)\Big|^2 \\ &= \Big|\sum_i U_{fi}^* U_{f'i} e^{-i\frac{m_i^2}{2E}L}\Big|^2 \\ &= \sum_{i=1}^{3}\sum_{j=1}^{3} U_{fi}^* U_{f'i} U_{f'j}^* U_{fj} e^{-i\frac{\Delta m_{ij}^2}{2E}L}, \end{aligned} \tag{3.7}$$

where standard notation $\Delta m_{ij}^2 = m_i^2 - m_j^2$ was used. After a little bit of mathematics the last expression can be rewritten in the following form

$$P_{\nu_f \to \nu_{f'}}(L,E) = \delta_{ff'} - 4\sum_{i>i'} \mathfrak{Re}(U_{fi}U_{fi'}^* U_{f'i'}^* U_{f'i}) \sin^2\Big(\frac{\Delta m_{ij}^2}{4E}L\Big) +$$

[6] Natural units are used everywhere.

$$+ 2\sum_{i>i'} \mathfrak{Im}(U_{fi}U^*_{fi'}U^*_{f'i'}U_{f'i}) \sin\Big(\frac{\Delta m^2_{ij}}{2E}L\Big). \tag{3.8}$$

It is worth noting that the oscillation probabilities depend on neutrino mass difference squared, therefore all neutrino oscillation experiments are sensitive only to Δm^2_{ij}. Also, in the case of a CP violation phase $\delta = 0$ the last term in (3.8) disappears and the oscillation probabilities are identical for neutrinos and antineutrinos. For the purpose of the experiment it is convenient to have the last equation when Δm_{ij}, E and L are expressed in eV^2, GeV and km respectively

$$\frac{\Delta m^2_{ij}}{2E}L \quad \rightarrow \quad 1.27\frac{\Delta m^2_{ij}[eV^2]}{E[GeV]}L[km] = \Delta_{ij}. \tag{3.9}$$

The probabilities which are being measured by the NOνA experiment are the probabilities of muon neutrino disappearance and electron neutrino appearance

$$P_{\nu_\mu\rightarrow\nu_\mu}(L,E) \approx 1 - \sin^2 2\theta_{23}\sin^2\Delta_{32}, \tag{3.10}$$

$$P_{\nu_\mu\rightarrow\nu_e}(L,E) \approx P_{atm} + P_{sol} + 2\sqrt{P_{atm}P_{sol}}(\cos\Delta_{32}\cos\delta \mp \sin\Delta_{32}\sin\delta), \tag{3.11}$$

with

$$P_{atm} = \sin^2\theta_{23}\sin^2 2\theta_{13}\sin^2\Delta_{31}, \qquad P_{sol} \approx \cos^2\theta_{23}\cos^2\theta_{13}\sin^2 2\theta_{12}\Delta^2_{21}, \tag{3.12}$$

where the "-" sign in 3.11 is for the neutrino and the "+" sign is for the anti-neutrino.

3.3 Oscillations in Matter

Each neutrino studied by the NOνA experiment travels through the Earth's crust for more than 810 km. While propagating through matter, neutrinos interact with medium constituting particles which leads to changes in neutrino oscillations. Since interaction going through exchange of only weak gauge bosons there are two types of possible interaction: (i) neutrino emits Z boson - neutral current (NC) interaction and (ii) neutrino emits $W^\pm$ boson - charged current (CC) interaction. In matter all three flavors of neutrinos interact through exchange Z boson with electrons, protons and neutrons.

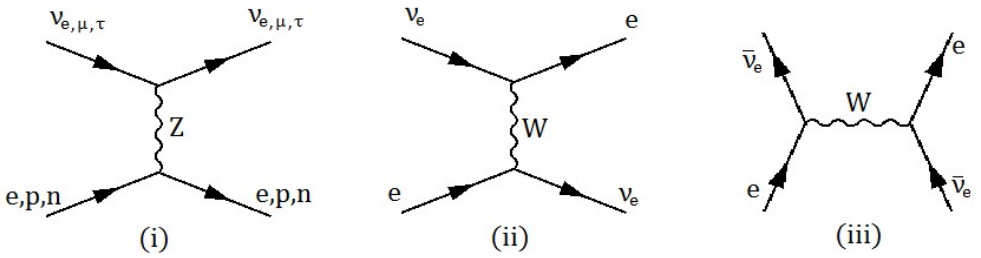

Figure 3.2: Neutrino interaction with matter. (i) All neutrinos participate in NC interactions which leads to additional effective mass for all eigenstates ν_1, ν_2 and ν_3, (ii) Additional CC interaction for electron neutrino ν_e, which modifies mass square difference, (iii) effect similar to (ii) only for electron anti-neutrino $\bar{\nu}_e$. The diagram (iii) contributes with opposite sign in comparison to (ii).

But only for electron neutrino there is another possibility - interaction through exchange W^+ boson with electrons as can be seen in the figure 3.2.

Accounting for interactions between neutrinos and all matter found on Earth adds two additional terms to the Hamiltonian which describes neutrino propagation - effective potential,

$$V_C = \sqrt{2} G_F N_e \qquad and \qquad V_N = -\frac{1}{\sqrt{2}} G_F N_n, \tag{3.13}$$

where G_F is Fermi constant, N_e and N_n electron and neutron number density respectively. The second term effectively shifts all $m_i^2 \to m_i^2 + 2|\mathbf{p}|V_N$ and does not have an effect on Δm_{ij}. The first term V_C enters the Hamiltonian in a such way that it has an influence only on the electron neutrino ν_e, and has the opposite influence on electron anti-neutrino $\bar{\nu}_e$. After further calculations one can derive the following corrected expressions for Δm_{32} and $\sin 2\theta_{13}$ in the presence of matter

$$\begin{aligned} \Delta m_{32}^2\Big|_{mat} &= \sqrt{(\Delta m_{32}^2 \sin 2\theta_{13})^2 + (\Delta m_{32}^2 \cos 2\theta_{13} \mp 2E_\nu V_C)^2} \\ \sin 2\theta_{13}\Big|_{mat} &= \frac{\Delta m_{32}^2 \sin 2\theta_{13}}{\sqrt{(\Delta m_{32}^2 \sin 2\theta_{13})^2 + (\Delta m_{32}^2 \cos 2\theta_{13} \mp 2E_\nu V_C)^2}} \end{aligned} \tag{3.14}$$

The matter effect has a significant influence on ν_e appearance probability and in the

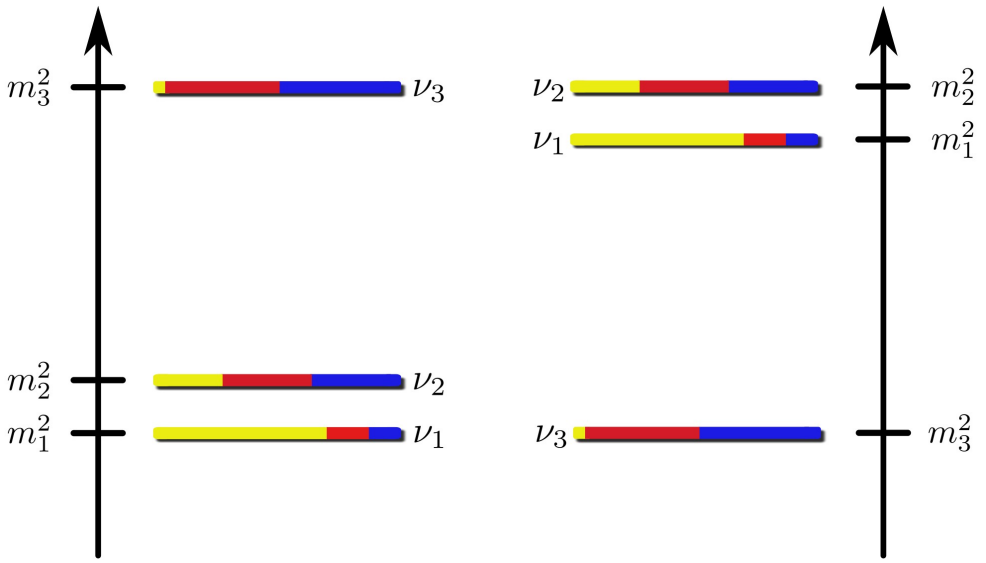

Figure 3.3: Two possible variants of neutrino mass hierarchies. The left side corresponds to the normal hierarchy (NH) and right side corresponds to the inverted hierarchy (IH). Colors represent how much and what kind of neutrino flavors contribute to every mass state. The electron flavor is yellow, muon flavor is red and the tau flavor is blue.

first approximation

$$P_{\nu_\mu \to \nu_e}(E,L)\Big|_{mat} = \Big(1 \pm \frac{2E_\nu V_C}{\Delta m^2_{32}}\Big) P_{\nu_\mu \to \nu_e}(E,L), \tag{3.15}$$

where the "+" sign is for the neutrino and the "-" sign is for the antineutrino. This effect is known as the Mikheyev-Smirnov-Wolfenstein (MSW) effect, and for the NOνA experiment it plays an important role in helping to determine the CP violating phase δ_{CP}.

It is worth noting that assigning specific masses to specific mass states are completely arbitrary, but it is known from experimental data that two masses are much closer to each other in comparison with the third mass. These two masses are called m_1 and m_2, with $m_2 > m_1$ and $\Delta m_{12} << |\Delta m_{32}| \approx |\Delta m_{31}|$. However, the sign of Δm_{32} is still unknown. That leaves two possibilities which are called normal hierarchy (NH) and inverted hierarchy (IH). Figure 3.3 illustrates the neutrino mass distributions. The NOνA experiment will be able to determine which hierarchy is realized in nature.

Chapter 4

The NOvA Experiment

The neutrinos studied by NOvA begin at Fermi National Accelerator Laboratory (Fermilab) in Illinois. An intense muon (anti-)neutrino beam is created at Fermilab by the Neutrino at the Main Injector (NuMI) source. NOvA, which stands for NuMI Off-Axis ν_e Appearance, is a long baseline experiment which is designed to determine the neutrino mass hierarchy, the octant of θ_{23}, and to measure the CP violating phase δ_{CP} by measuring electron (anti-)neutrino appearance probability and muon (anti-)neutrino disappearance. It consists of the Near Detector (ND), which is located at Fermilab and measures total flux of neutrino, and the Far Detector (FD), which is located near Ash River, Minnesota and measures flux of muon and electron neutrinos. The structures of the NuMI source and the Near and Far Detectors, and the detector positions relative to the beam axis will be explained in the following sections.

4.1 NuMI and Off-Axis Detectors Position

Neutrinos for the NOvA experiments comes from decay of pions and kaons. To get a beam of the mesons Main Injector at Fermilab is used, which provides an intense beam of proton with energy 120 GeV. The structure of NuMI is illustrated on figure 4.1. It is designed to deliver 4.9×10^{13} proton on target (POT) with the repetition rate of 1.3s, which corresponds to 700 kW of beam power. The proton beam is directed into a graphite target. Collisions between the proton beam and graphite target produces many types of hadrons and mesons, with pions and kaons among them. Magnetic focusing

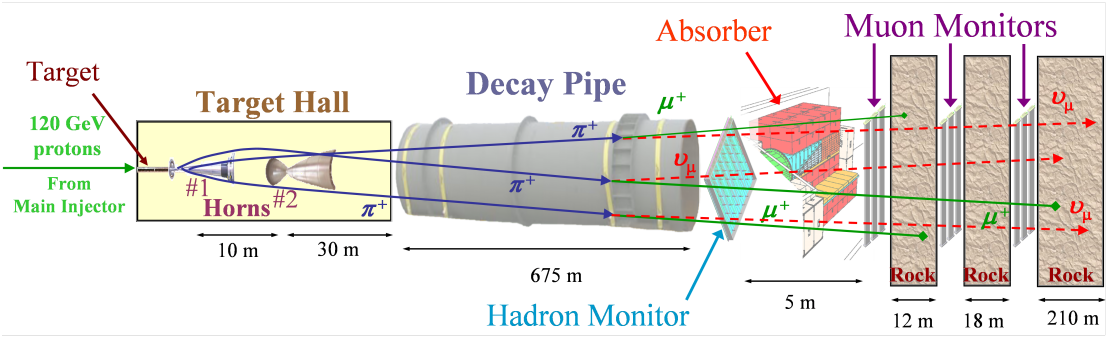

Figure 4.1: Schematics of neutrino production[1].

horns, which are supplied with current of 200kA, are used to focus and direct charged pions and kaons into a decay pipe. The decay pipe is long enough such that nearly all of the incoming pions and kaons decay before the end of the pipe. More than 99% of all pions and 63% of kaons decay into anti-muon/muon and muon/anti-muon neutrino, so the flux of particles at the end of the decay pipe consists of mostly muons and muon anti-neutrinos, or their antiparticles. By changing the electric current direction in the focusing horns one can switch between positively and negatively charged pions and kaons which enter the decay pipe. This gives an opportunity to make two types of neutrino beams - ν_μ's and $\bar{\nu}_\mu$'s. Unfortunately, 5% of charged kaons have electron neutrinos among their byproducts, and this is an irreducible background for an electron neutrino analysis. All the realitively long lived charged particles such as muons and electrons do not reach Near Detector as they get absorbed in rock. A hadron monitor, absorber and muon monitor are placed at the end of decay pipe to better understand beam properties, but they do not play any role in the NOvA experiment.

After the neutrinos leave the decay pipe they begin their journey to the near and far detectors. There are a few reasons why the NOνA detectors are placed 14.6 mrad off-axis of the NuMI beam. As can be seen on the picture on the right, the first minimum of muon neutrino survival probability and first maximum of electron

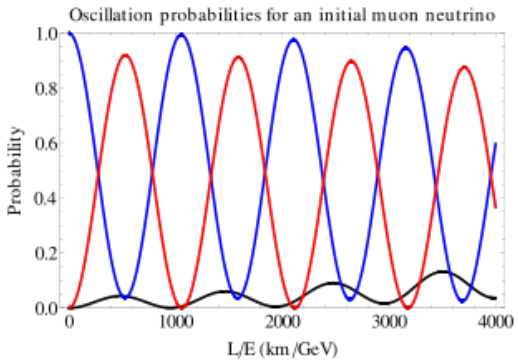

neutrino appearance probability are around 400 km/GeV but on-axis neutrino spectrum (black line on left picture 4.2) does not allow to observe first maximum of $P(\nu_\mu \to \nu_e)$ for a baseline 1000 km. The solution is simple: pions and kaons decay isotropically in their rest frame but after Lorentz boost to laboratory frame flux and neutrino energy at the far detector (for small off-axis angles θ) can be expressed in the following form

$$F = \Big(\frac{2\gamma}{1+\gamma^2\theta^2}\Big)^2 \frac{A}{4\pi d} \tag{4.1}$$

$$E_\nu = \frac{0.43 E_\pi}{1+\gamma^2\theta^2}, \tag{4.2}$$

where $\gamma = \frac{E_\pi}{m_\pi}$, A is the size of the detector front area and d is the distance to the detector. For kaons numerical factor 0.43 should be changed to 0.96. Knowing the pion and kaon energy spectrum at the NuMI source, one can predict the neutrino energy spectrum at the far detector for different off-axis angles θ. As shown on left side of Figure 4.2, the neutrino energy distribution gets narrower and shifts toward smaller energies. At 14.6 mrad the neutrino flux is still moderate and peaked near 2 GeV, which allows NOvA to study the region of maximal $P(\nu_\mu \to \nu_e)$ at 810 km. Moreover, the narrow peak decreases the chance that NC events from more energetic neutrinos could be misidentified as CC events in the energy region of interest. In general, the off-axis detector placement significantly improves the sensitivity of the probability measurement.

4.2 NOvA Near and Far Detectors

The NOvA experiment utilizes two detectors for measuring muon neutrino disappearance probability $P(\nu_\mu \to \nu_\mu)$ and electron neutrino appearance probability $P(\nu_\mu \to \nu_e)$. In order to decrease systematic uncertainties, such as beam uncertainty and uncertainties due to variation in detector efficiency, two detectors are build with exactly the same material and similar geometry. The Near Detector is placed 1 km from the NuMI source at Fermilab, while the Far Detector sits 810 km away on the surface and 14.6 mrad off beam axis in Ash River, Minnesota. The Near Detector weighs 330 metric ton and is 105 m underground, while the Far Detector mass is 14,000 ton and has shielding equivalent

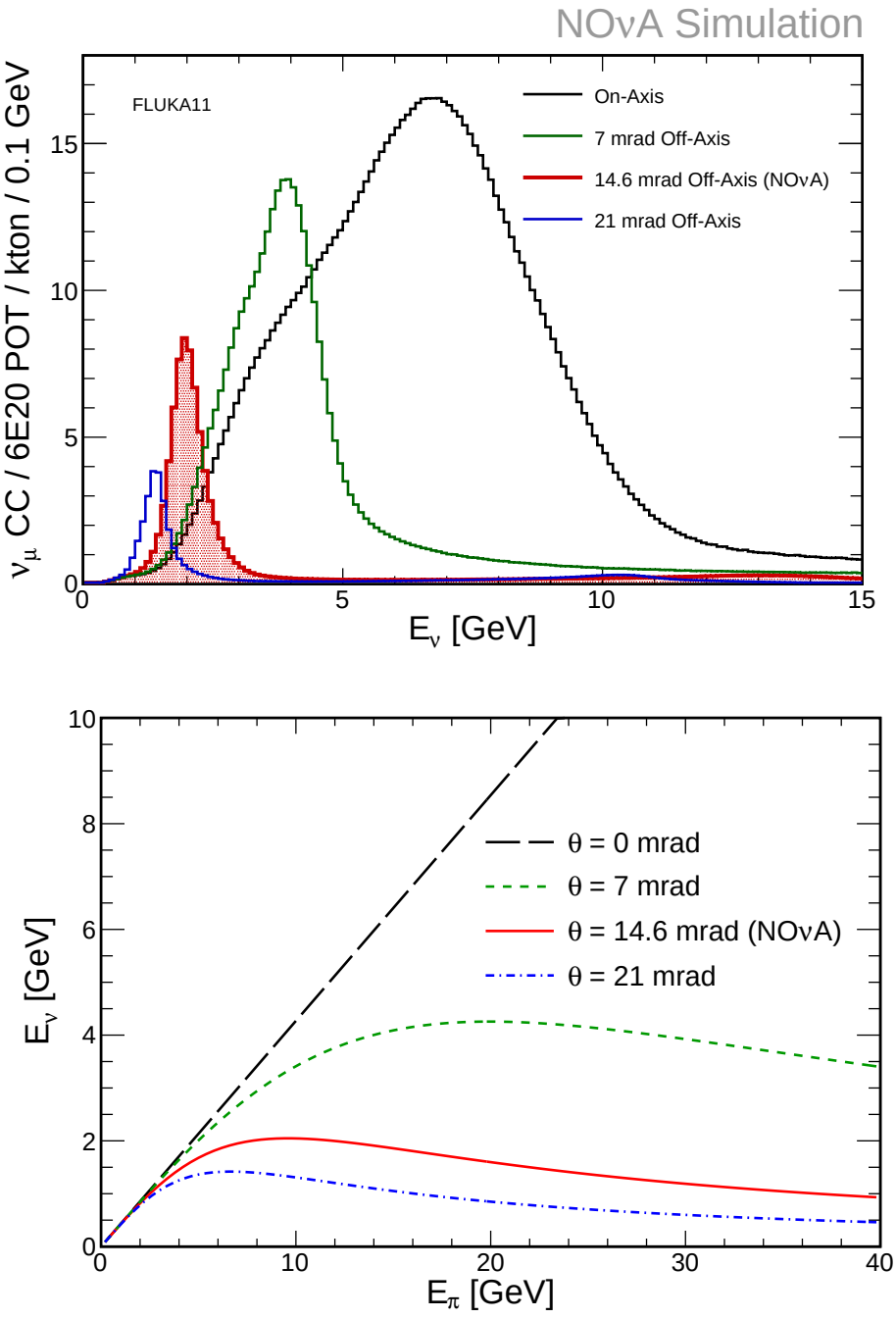

Figure 4.2: (Left) Expected unoscillated neutrino spectrum at the Far Detector as a function of angle relative to NuMI beam. (Right) Neutrino oscillation probabilities as a function of $\frac{L}{E}$, $P(\nu_\mu \to \nu_\mu)$ - blue line, $P(\nu_\mu \to \nu_e)$ - black line and $P(\nu_\mu \to \nu_\tau)$ - red line.

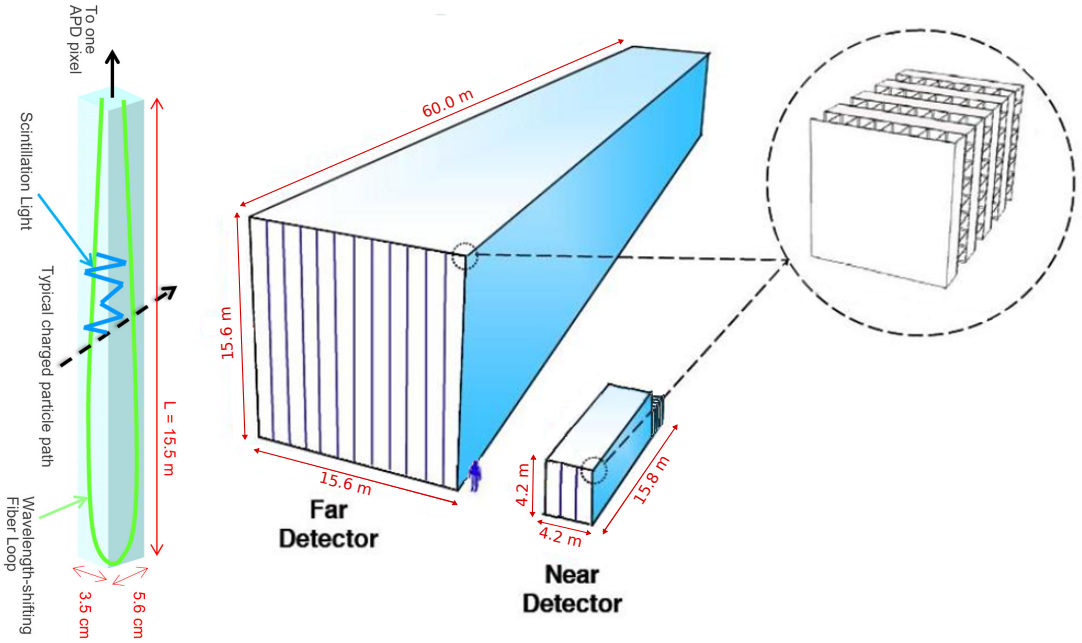

(a) A NOvA cell

(b) Scale and structureof the NOvA detectors

Figure 4.3: Structure of cell and the NOvA detectors

to 3 m of rock which reduces cosmic ray background.

4.2.1 From cells to planes and blocks

Each detector is made of cells which are made from polyvinyl chloride (PVC) doped with titanium dioxide to increase light reflectivity. The cross section of cells has rectangular shape with sizes approximately equal to 4 cm and 6 cm. The length of the cells is varies between the detectors and equals to 4 m for the Near Detector and 15 m for the Far Detector. 32 cells are bound together along 6 cm side to make a module and the set of modules produces plane. The number of modules in a plane depends on a detector - 3 and 12 modules per plane for the Near and Far Detector respectively. Planes are glued together in a such way that adjacent planes alternating between horizontal and vertical allignment. The scetch of the detectors structure can be seen in 4.3b. Furthemore, 32 planes make up a block and 28 blocks complete the full Far Detector while for the Near Detector block consists of 24 planes and 3 blocks make the active part of the detector. In addition, so called muon catcher block goes upstream and serves for stopping muons

which are produced in ν_μ CC interactions. Muon catcher, which helps to contain more muons as the relative size of the Near Detector is not big, consists of 22 active planes together with 10 steel 10 cm thick planes between every 2 active ones. The size of the muon catcher in XY plane is smaller the the active part of the Near Detector since horizontal planes have only 2 modules while vertical planes have 3 modules. The presents of the steel leads to extra muon energy absorbtion which makes muon tracks shorter.

Planes configuration allows to reconstruct three-dimensional tracks of the particles; vertical cells provide X measurements, horizontal cells give Y measurements, and planes positions provides Z measurements. Z-axis is directed along the beam, X-axis points to the west and Y-axis points upward. This choice of axes gives NOvA detectors a Cartesian right handed coordinate system.

4.2.2 Signal path part I: ligth production and digitization

In order to detect particles resulted in neutrino interactions in the detectors these particles should leave footprints. In NOvA experiment cells are filled with a liquid scintillator composed of mineral oil doped with pseudocumene [1]. In every cell, one wavelength shifting fiber runs from one end of the cell to the opposite end, then back to the other end where it connects to an avalanche photodiode (APD) as can be seen in 4.3a. Photons are created by charged particle moving through the scintillator. These reflected by the cell walls and have a high chance to be captured by the wavelength shifting fiber. Inside the fiber photons after absorbtion and reemission increse its wavelength resulting in propogation without escaping due to total inner reflection.

Photons which reach APD get converted into photoelectrons through the process called avalanche breakdown, and produces currents which are detectable by commercial electronics. All 32 fiber from the module are connected to one APD. And the last step before signals might be processed with the help of conventional computers is to digitize the APD output signal. The digitization happens in front end board (FEB). Short APD signals are stretched in time in the Application Specific Integrated Circuit (ASIC) with the help of CR-RC circuit. After, the signal is passed to ADC - analog to digital converter - where continuous signal is translated to discrete one with 4096

[1] 1,2,3-Trimethylbenzene

distinct values. Every channel is read out every 500 ns and 125 ns for the Far and Near Detector respectively. Only the 4 last ADCs - value of the digitization sample - are stored as a hit and the hit is written when the difference

$$ADC_i - ADC_{i-3} \tag{4.3}$$

is greater than a threshold. These 4 values are then passed to the Data Concentration Module (DCM). Later, those 4 values are used to fit the signal shape and to determine signal amplitude, which is proportional to amount of energy charged particle deposited in a particular cell.

4.2.3 Signal path part II: data acquisition

Every DCM is a custom built computer and collecting data from 64 FEBs. When infromation from FEBs is time sorted and arrange in 5 ms chunk of data stream, the data is sent to a buffer node where it stored until a trigger decision is made if the data needs to be saved to the disks. 200 buffer nodes are arranged in a circular ring buffer and every node has up to a minute to run a trigger software until a new piece of data comes from a DCM. NOvA trigger software which issues trigger decisions relies on external triggers as well as data-drivien triggers based on recieved data. Neutrino oscillation analysis uses data which is recorded due to external trigger desicions, this so-called NuMI trigger is issued by acceleration complex at Fermilab. The trigger records 550 μs window of data centered around the 10 μs NuMI beam spill. There are several more triggers such as cosmic trigger, which triggers at the rate of 10 Hz to store FD cosmic data for callibration and background estimation, or supernova trigger, which ideally should record up to 20 minutes of data in the event of supernova burst.

Recorded data is stored at the FD and ND cites. However, there are no enough disk space at the cites and eventually all the data is transferred to Fermilab where it is processed further for the physics analysis.

4.2.4 Neutrino Interactions in NOvA

The majority of neutrinos at the NOvA detectors are in the few GeV energy region and all the charged products of neutrino interaction with a nucleus are clearly visible and as

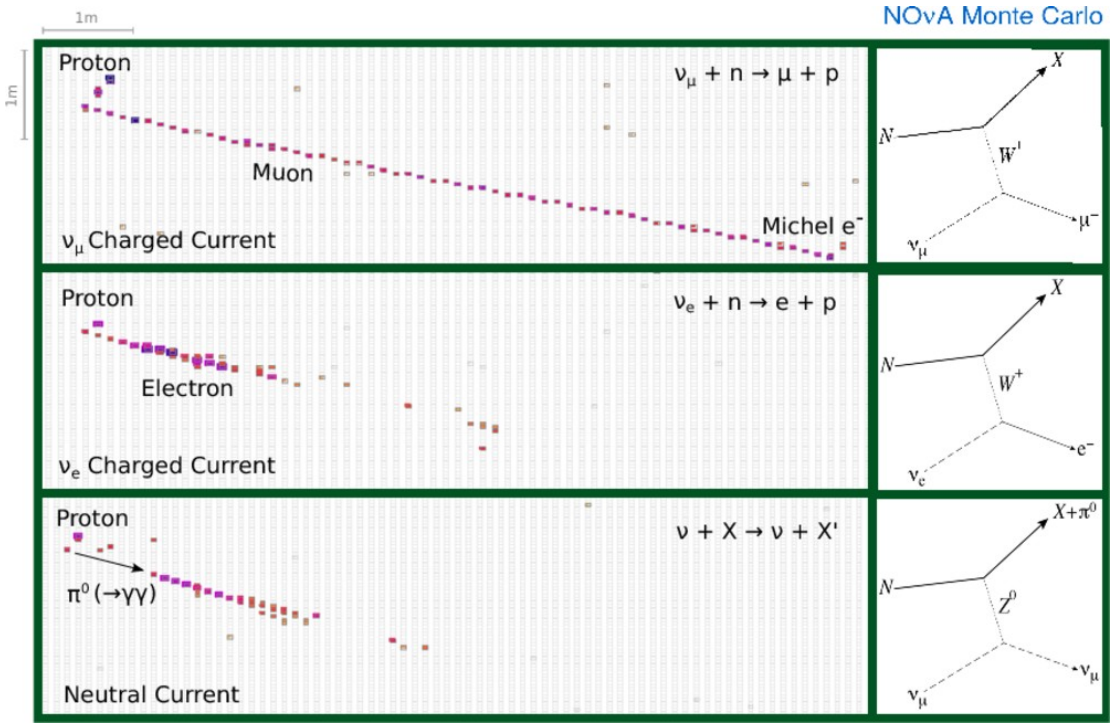

Figure 4.4: Neutrino interactions in NOvA detectors.
Three types of neutrino interactions are shown. The top part shows ν_μ CC interaction with some proton activity and long muon track left by high energy muon. The middle part shows ν_e CC interaction, electron develops a long electromagnetic shower with radiation length being much bigger than Moliere radius. The bottom part shows neutrino NC interaction with π^0 among the resulting particles which later produces an electromagnetic shower by decaying into two photons. NC type events form a primarily background in ν_e disapperance analysis.

long as their momenta are sufficiently separated in an angular space. As can been seen in 4.4 muons, electrons, and charged hadrons leave a distinct traces in NOvA. Particles primary lose their energy through an ionization process by disrupting electrons of atoms which happen to be close to particles trajectories. Being much havier than an electron and immune to a strong interaction muon can travel a long distance inside the detectors which make it a relatively easy task to determine a high energy muon. Light electron interacts with detector material via pair production and forms electromagnetic shower, where energy is depossed in a rather conical shaped region as opposed to a long muon track. Hadrons such as protons and pions in addition to ionization also lose energy by interacting strongly with nuclei along their trajectory.

Despite these differences it is a complicated problem to distinguish a charged current (CC) interaction with muon or electron been produced from a neutral current (NC) one where no visible lepton is produced. NC processes can output charged or neutral pions together with other hadrons. Charged pions leave tracks which could be confused with low energy muons, although occasional hard scatters of the nuclei help with identification. Neutral pions leave electromagnetic showers after they decay into two photons and these showers might be confused with showers created by electrons in CC neutrino interaction. Thus, sophisticated algorithms need to be developed to measure parameters of neutrino mixing matrix where determination of exact neutrino flavor is a crucial task.

In addition, since NOvA Fad Detector sits on the ground it constantly being bombarded by muons and other particles created by interactions of cosmic rays - high energy protons - with air molecules in upper atmosphere. These muons contribute to a background for the main analysis but they could be relatively easy to get rid off because of their activity at the top and/or at the sides of the detector. However, they are much harder to deal with since cosmic muons a primarily background in a uncontained sample which this thesis are partially about.

4.2.5 NOvA Event Display

The NOvA event display helps to visualize a real data gathered by the detectors or a simulated one. The result of ν_μ CC interaction measured on April 22, 2014 is shown in 4.5. As NOvA detectors consist of alternating horizontal and vertical planes, event

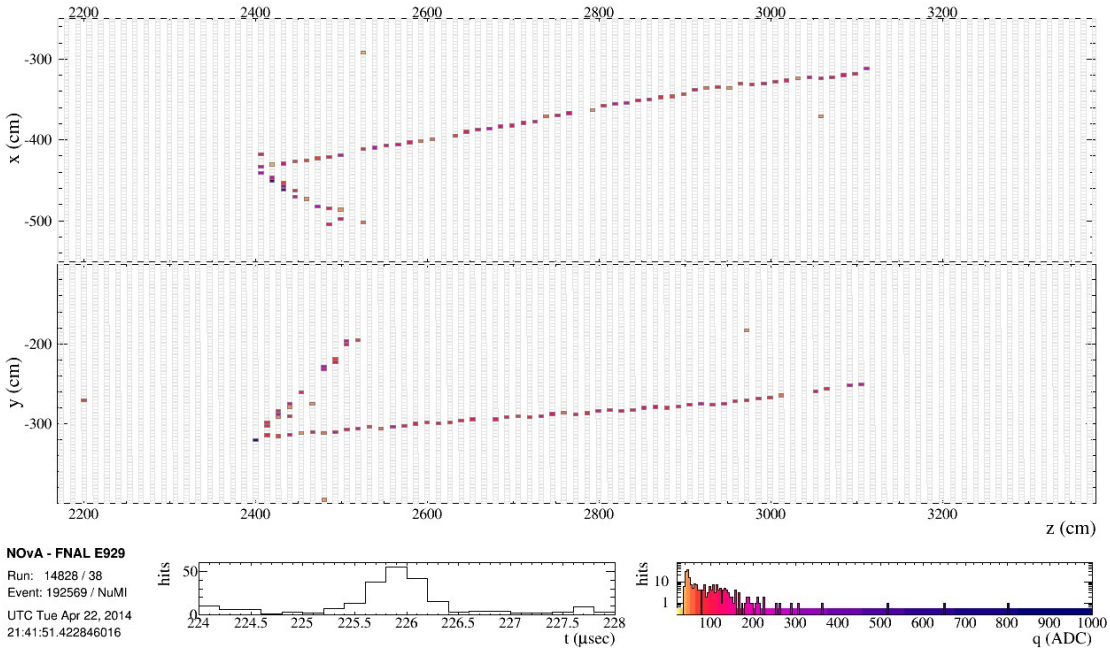

Figure 4.5: NOvA Event Display.
The candidate ν_μ CC event at the Far Detector zoomed in space and time. Top and bottom windows show X-Z and Y-Z projections.

display shows hits from two types of planes in a separate windows. The top window displays X-Z hits position (detector activity as seen from the top), while the lower one displays Y-Z hits position (detector activity as seen from the side). The software allows to change a spatial zoom as well as a time zoom to see closely activity he/she might be interested in. Hits time distribution and deposited photoelectron charge distribution in ADC units together with event time stamp and trigger information are shown below the main windows. Hits also could be colored by their time, to see if they are close to readout window or not, or by their deposited charge, to see where the most of the energy was deposed. In the shown example, hits are colored by their charge.

Chapter 5

Simulation

In order to predict spectra at the near and the far detectors to compare predictions with actual data one need to simulate neutrino interactions in the detectors relying on known physics models and theories of how particles are produced, how they travel and interact with detector material. The simulation process in the NOvA starts with protons hiting NuMI target and finishes with APD readouts and analog to digital converters. Side simulation packages or custom NOvA software are used in every step, output information on every step is used as input data for the following step

- Beam simulations. FLUGG simulation package which is the combination of FLUKA [19] and GEANT4 [20] packages. Geometries of the target hall and detectors are encoded with the help of GEANT4, while proton interactions and downstream particle decays are simulated with FLUKA.

- Neutrino interactions. Neutrino flux degenrated in the previous step is an input for the GENIE [21] package, which performs simulation of neutrino interactions with nucleus inside the detectors. GENIE produces a list of particles leaving the nucleus.

- Propagation of particles through detectors. List of the particles and detailed detectors geometry are used by GEANT4 to simulate particles propagation through the detectors. Amount of energy deposited by the particles in every cell is the input for the last step.

- Electronic signal. Deposited energy in the cell is converted to a light by the scintillator which travels through the fiber to an APD and analog to digital converter. This step is simulated by NOvA custom software [22].

All these 4 parts will be briefly discussed in the current chapter.

5.1 Beam Simulation

Beam simulation provides NOvA experiment with neutrino flux prediction at both detectors. This simulation is done by FLUKA and GEANT4 through the FLUGG interface. Detailed geometry of the target hall, target itself, collimator, two focusing horns and decay pipe is described by GEANT4 format files and simuation is done by FLUKA. The FLUKA package simulates 120 GeV protons which hit the target and give rise to hadronic showes, secondary particles focused by the horns and enter decay pipe where they further decay and some of them produce neutrinos. All the proton interaction information whose dauther particles produce neutrino is saved providing a way to study beam uncertanties related to particle production models.

The simulation outputs files which describe neutrino flux in terms of neutrino parent particles, flavour, energy and direction of motion.

5.2 Simulation of Neutrino Interactions

In order to simulate neutrino interactions in the near and far detector the GENIE simulation package is used. The package is developed by the experimental physics community and serves as a primary neutrino Monte Carlo generator for neutrino experiments due to its ability to simulate neutrino interactions on almost any target and in wide energy region which spans from MeV to PeV. As mentioned above GENIE gets a result of neutrino flux simulation from a previous step and convolute it with neutrino interaction cross sections.

The interesting feature of the neutrino energy spectrum in NOvA experiment is that it overlaps with energy regions of several neutrino interaction models. All these models are implemented in GENIE simulation package. Quasi-Elastic scattering (QE), deep-inelastic scattering (DIS), baryon resonance production (RES) as well as meson exchange

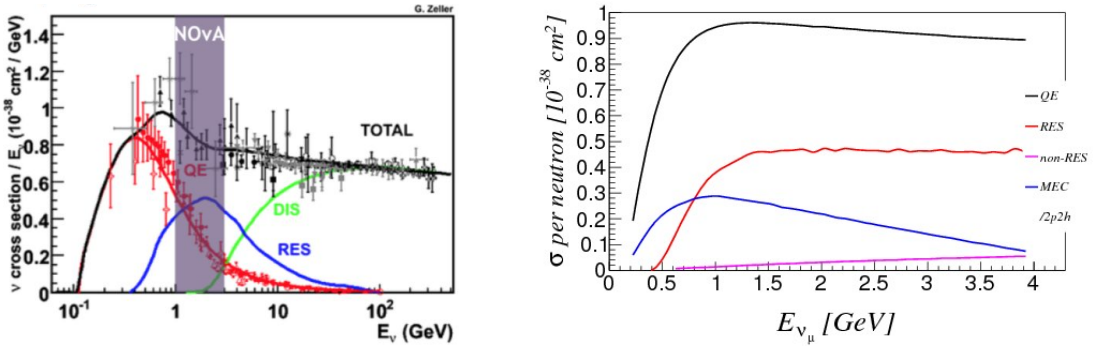

(a) Neutrino cross section energy dependence for QE, RES and DIS intercations overlapped with NOvA energy region used for the oscillation analysis.

(b) Neutrino cross section energy dependence used in GENIE neutrino generator.

current (MEC) which dominates in 2 particle - 2 hole (2p-2h) effect. The physics behind the models is complicated, however on the qualitative level QE interaction means scattering off a single nucleon, MEC interaction means scattering off a pair of nucleons, RES process results in excitation of the whole nucleus and DIS interaction of neutrino with a nucleus can lead to a complete disintegration of the nucleus[1].

On the left hand side of 5.1a one can see a typical energy regions of QE, RES and DIS neutrino interactions overlaped with NOvA energy domain. These three types of neutrino scattering are implemented in GENIE based on the Llewellyn-Smith model [23], Rein-Sehgal model [24] and effective leading order model with Bodek and Yang modifications [25] for QE, RES and DIS respectively. MEC process, which is included in GENIE as semi-empirical model, is described in [26].

5.3 Particles propagation

After GENIE is done with its part of simulation, or in other words, the list of particles which leave the nucleus with their energies, momenta and initial positions is ready, now one needs to propagate them through the detector material and simulate the energy deposition, interaction and decay. NOvA experiment uses GEANT4 [20] simulation package for this step. Besides the list of particles, GEANT4 takes another input namely

[1] This happens when energy transferred to a nucleus is sufficiently large

geometry of the detector and its surrounding. Detailed information about blocks positions, cell structure and materials they made of, scintillator composition, conrete and steel support structure around the detectors is encoded in special geometry files.

The way GEANT4 propagates particles is done in the following manner. For each particle at each step of the trajectory it is decided with appropriate probability what particle should do next - move forward and deposit some energy, interact and scatter of particles which constitute detector components or decay. As particle propagates further it loosing its kinetic energy and as soon as particle's kinetic energy is less than 100 eV propagation stops. GEANT4 saves these trajectory steps as a list of particle positions, energy and momenta for the next step of simulation chain.

Before the final detector response could be simulated it is necessary to determine how much light was produced in the scintillator and what fraction of it was collected by the wave-shifting fiber and transported to the readout electronics. As a matter of fact, amount of light produced by the scintillator is not linearly proportional to amount of deposited energy due to a finite number of scintillaotr centres along the particle trajectory in the cell. The effect is know as Birks supression [27]. If $\frac{dL}{dx}$ is light output per unit length and $\frac{dE}{dx}$ is amount of deposited energy then Birks law reads

$$\frac{dL}{dx} = L_0 \frac{\frac{dE}{dx}}{1 + k_B \frac{dE}{dx}}, \tag{5.1}$$

where L_0 and k_B are constants which depend on scintillator. However, more carefull aproach to the problem of particle propagation through scintillator was carried out by Chou [28] and additional correction was introduced to the Birks law. NOvA experiment utilizes this correction -

$$\frac{dL}{dx} = L_0 \frac{\frac{dE}{dx}}{1 + k_B \frac{dE}{dx} + k_C \left(\frac{dE}{dx}\right)^2}. \tag{5.2}$$

Parameters k_B and k_C are tuned using muon and protons tracks in the Near Detector.

Chapter 6

Event Reconstruction

Chapter 7

Data Analysis Strategy

Chapter 8

ν_μ CC Selection

Chapter 9

Analysis

9.1 Analysis Procedure

9.2 Analysis Result

Chapter 10

Systematics

Chapter 11

Conclusion and Discussion

In this chapter we will briefly summarize our results! Or maybe not! Or maybe yes! QQWQWWQQQW

References

[1] R. Zwaska. *Accelerator systems and instrumentation for the NuMI neutrino beam.* PhD thesis, University of Texas, 2005.

[2] J. Chadwick. Intensitatsverteilung im magnetischen spektren der β-strahlen von radium b + c. *Verh. Dtsch. Phys. Ges.*, 16:383, 1914.

[3] W. Pauli. Open letter to the group of radioactive people at gauvereins meeting in tubingen, 1930.

[4] J. Chadwick. The existence of a neutron. *Royal Society of London Proceedings Series A*, 136:692, 1932.

[5] E. Fermi. Versuch einer theorie der β-strahlen. i. *Zeitschrift fur Physik*, 88:161, 1934.

[6] C. L. Cowan Jr., F. Reines, F. B. Harrison, H. W. Kruse, and A. D. McGuire. Detection of the free neutrino: A confirmation. *Science*, 124:103, 1956.

[7] G. Danby, J-M. Gaillard, K. Goulianos, L. M. Lederman, N. Mistry, M. Schwartz, and J. Steinberger. Observation of high-energy neutrino reactions and the existence of two kinds of neutrinos. *Phys. Rev. Lett.*, 9:36, 1962.

[8] G. Arnison et. al. (UA1 Collaboration). Experimental observation of isolated large transverse energy electrons with associated missing energy at $s = 540$ gev. *Physics Letters B*, 122:103, 1983.

[9] G. Arnison et. al. (UA1 Collaboration). Experimental observation of lepton pairs of invariant mass around 95 gev/c^2 at the cern sps collider. *Physics Letters B*, 126:398, 1983.

[10] D. DeCamp et. al. (ALEPH Collaboration). Determination of the number of light neutrino species. *Physics Letters B*, 231:519, 1989.

[11] M. L. Perl et. al. Evidence for anomalous lepton production in e^+e^- annihilation. *Physical Review Letters*, 35:22, 1975.

[12] K. Kodama et. al. (DONUT Collaboration). Observation of tau neutrino interactions. *Physics Letters B*, 504:218, 2001.

[13] B. Pontecorvo. Mesonium and antimesonium. *Zhur. Eksptl. i Teoret. Fiz.*, 1957.

[14] Z. Maki, M. Nakagawa, and S. Sakata. Remarks on the unified model of elementary particles. *Prog. Theor. Phys.*, 28:870, 1962.

[15] R. Davis, D. Harmer, and K. Hoffman. Search for neutrinos from the sun. *Phys. Rev. Lett.*, 20:1205, 1968.

[16] John N. Bahcall. Solar neutrino cross sections and nuclear beta decay. *Phys. Rev. B*, 135:137, 1964.

[17] Y. Suzuki. Kamiokande and super-kamiokande. *Progress in Particle and Nuclear Physics*, 40(0):427, 1998.

[18] A. B. McDonald et. al. (SNO Collaboration). First neutrino observations from the sudbury neutrino observatory. *Nuclear Physics B - Proceedings Supplements*, 91(13):21, 2001.

[19] A. Fasso, A. Ferrari, J. Ranft, and P. R. Sala. FLUKA: Present status and future developments. *Conf. Proc.*, C9309194:493–502, 1993.

[20] S. Agostinelli et al. GEANT4: A Simulation toolkit. *Nucl. Instrum. Meth.*, A506:250–303, 2003.

[21] C. Andreopoulos et al. The GENIE Neutrino Monte Carlo Generator. *Nucl. Instrum. Meth.*, A614:87–104, 2010, 0905.2517.

[22] A Aurisano, C Backhouse, R Hatcher, N Mayer, J Musser, R Patterson, R Schroeter, and A Sousa. The nova simulation chain. *Journal of Physics: Conference Series*, 664(7):072002, 2015.

[23] C. H. Llewellyn Smith. Neutrino Reactions at Accelerator Energies. *Phys. Rept.*, 3:261–379, 1972.

[24] Dieter Rein and Lalit M. Sehgal. Neutrino Excitation of Baryon Resonances and Single Pion Production. *Annals Phys.*, 133:79–153, 1981.

[25] R. P. Feynman, M. Kislinger, and F. Ravndal. Current matrix elements from a relativistic quark model. *Phys. Rev.*, D3:2706–2732, 1971.

[26] T. Katori. Meson exchange current (mec) models in neutrino interaction generators. *AIP Conf. Proc.*, 1663:030001, 2015.

[27] J B Birks. Scintillations from organic crystals: Specific fluorescence and relative response to different radiations. *Proceedings of the Physical Society. Section A*, 64(10):874, 1951.

[28] C. N. Chou. The nature of the saturation effect of fluorescent scintillators. *Phys. Rev.*, 87:904–905, Sep 1952.

Appendix A

Glossary and Acronyms

Care has been taken in this thesis to minimize the use of jargon and acronyms, but this cannot always be achieved. This appendix defines jargon terms in a glossary, and contains a table of acronyms and their meaning.

A.1 Glossary

- **Cosmic-Ray Muon** (**CR** μ) – A muon coming from the abundant energetic particles originating outside of the Earth's atmosphere.

A.2 Acronyms

Table A.1: Acronyms

Acronym	Meaning
CRμ	Cosmic-Ray Muon